

Enhanced Ozone Downscaling in Megacities Using a SHAP-Optimized U-Net Model

Ata A. Kakroodi¹, Hossein Barekati¹, Hamid Kiavarz Moghaddam²

¹ Department of Remote Sensing and GIS, Faculty of Geography, University of Tehran, Iran - a.a.kakroodi@ut.ac.ir, hossein.barekati@ut.ac.ir

² Geomatics Engineering, Department of Earth & Space Science & Engineering, York University, Toronto, Canada - hkiavarz@yorku.ca

Keywords: Ozone Downscaling; U-Net; SHAP; Urban Air Quality; High-Resolution Mapping.

Abstract

High-resolution mapping of tropospheric ozone is essential for urban environmental assessment; however, satellite-derived ozone products are generally too coarse to capture neighborhood-scale variability in complex megacities such as Tehran. This study introduces an interpretable deep-learning framework that downscales coarse Sentinel-5P ozone observations to a 30-m spatial grid by integrating a U-Net convolutional architecture with SHapley Additive exPlanations (SHAP). A diverse suite of predictors—including land-surface indicators, meteorological parameters, terrain morphology, and chemical precursors—was harmonized and resampled to a unified spatial resolution. SHAP analysis was applied to quantify each predictor's contribution, enabling the removal of redundant or low-impact variables before model training. Using spring 2020 as the evaluation period, the optimized U-Net successfully reconstructed fine-scale ozone gradients and reproduced Tehran's characteristic north-south pattern driven by topography and emission density. Comparative analysis with preliminary outputs demonstrates that feature optimization enhances spatial coherence, reduces noise artifacts, and improves the representation of localized hotspots. Statistical evaluation further showed strong agreement between the downscaled ozone estimates and observational data at both station and district scales, demonstrating effective generalization across heterogeneous urban environments. Overall, the findings highlight the potential of combining deep learning with interpretability techniques to refine coarse satellite ozone observations and provide a scalable, high-resolution framework for urban air-quality monitoring and exposure assessment.

1. Introduction

Urban ozone pollution has become a critical environmental concern in densely populated megacities, where complex interactions among topography, emission patterns, and meteorological dynamics create pronounced fine-scale spatial variability. Tropospheric ozone is recognized as one of the most important secondary air pollutants because of its adverse effects on human health, ecosystems, and climate systems (Donzelli & Suárez-Varela, 2024; An et al., 2024). Although satellite platforms such as Sentinel-5P/TROPOMI provide consistent global monitoring of tropospheric ozone, their coarse native resolution—typically several kilometers—limits their usefulness for neighborhood-level or intra-urban assessments (Geddes et al., 2022). This limitation is particularly evident in topographically constrained cities such as Tehran, where sharp elevation gradients, heterogeneous land-use patterns, and spatially uneven emission intensities result in highly variable ozone distributions across short distances (Ezimand & Kakroodi, 2019). Similar topography-driven ozone gradients have been reported in mountainous urban environments, where elevation, land-surface characteristics, and mountain-valley circulation strongly influence pollutant transport and accumulation (Seguel et al., 2013; Roldán et al., 2021; Afarideh et al., 2023).

To address the mismatch between coarse satellite observations and urban-scale information needs, numerous downscaling strategies have been proposed, ranging from statistical and geostatistical approaches (Gauthier et al.,

2022) to advanced machine-learning and deep-learning architectures such as Random Forests, XGBoost, and transformer-based hybrid models (Chen et al., 2025). Recent studies have further demonstrated the effectiveness of geostatistical, machine-learning, and hybrid approaches for enhancing the spatial resolution of satellite-derived air-quality products (Cheng et al., 2024; Chen et al., 2024; Lu et al., 2024). Among these techniques, the U-Net convolutional neural network has gained substantial attention owing to its encoder-decoder architecture, which effectively captures multiscale spatial features and preserves local spatial continuity while learning complex nonlinear dependencies from diverse environmental inputs (Li et al., 2020). However, despite its strong modeling capability, U-Net-based frameworks may incorporate redundant or weakly relevant predictors, which can reduce generalization performance, increase computational cost, and limit model interpretability.

To overcome these challenges, this study introduces a feature-optimized deep-learning framework that integrates U-Net with SHapley Additive exPlanations (SHAP). This hybrid approach enables the model to reconstruct high-resolution ozone patterns while simultaneously quantifying the marginal contribution of each predictor and eliminating low-impact variables prior to training, thereby enhancing robustness, interpretability, and computational efficiency (He et al., 2023; Ponce-Bobadilla et al., 2024). Leveraging a rich multi-source dataset—including land-surface indicators, topographic metrics, vegetation indices, meteorological variables, and chemical precursors—the framework generates 30-m ozone surfaces that capture both

seasonal dynamics and the underlying physical processes governing ozone formation in complex urban environments. Previous studies in Tehran have highlighted the strong spatio-temporal variability of ozone concentrations and the importance of incorporating urban and environmental factors into predictive models (Sherafati et al., 2022). Furthermore, recent machine-learning-based downscaling frameworks have demonstrated promising performance in generating high-resolution atmospheric pollutant maps from coarse satellite observations and multi-source geospatial datasets (Mamić & Pirotti, 2025; Shetty et al., 2025; Hu et al., 2024).

Overall, the proposed methodology aims to enhance coarse Sentinel-5P ozone observations and produce spatially detailed, physically consistent maps suitable for urban exposure assessment, environmental monitoring, and air-quality policy applications. Through the integration of deep learning and interpretable feature-importance analysis, this study establishes a scalable and transferable workflow for high-resolution atmospheric pollution mapping in data-scarce yet spatially heterogeneous megacities such as Tehran.

2. Study Area and Data

The study area encompasses the metropolitan region of Tehran, a topographically complex and densely urbanized environment extending from the elevated foothills of the Alborz Mountains in the north to the highly populated southern plains. This pronounced altitudinal gradient, combined with heterogeneous land-use patterns and substantial anthropogenic emissions, produces strong fine-scale variability in ozone formation across the city (Ezimand & Kakroodi, 2019). The contrast between the well-ventilated northern districts—characterized by higher elevations and stronger mountain–valley airflow—and the low-lying southern basins, where pollutant accumulation is more persistent, makes Tehran an ideal case study for evaluating high-resolution ozone downscaling performance. Similar topography-driven air-pollution gradients have also been documented in other mountainous megacities, where terrain complexity strongly influences atmospheric circulation, pollutant transport, and accumulation processes (de Foy et al., 2022).

As shown in Figure 1, Tehran exhibits a pronounced north–south elevation gradient and heterogeneous urban structure, with ozone monitoring stations distributed across its 22 municipal districts, providing a suitable framework for evaluating high-resolution ozone downscaling performance.

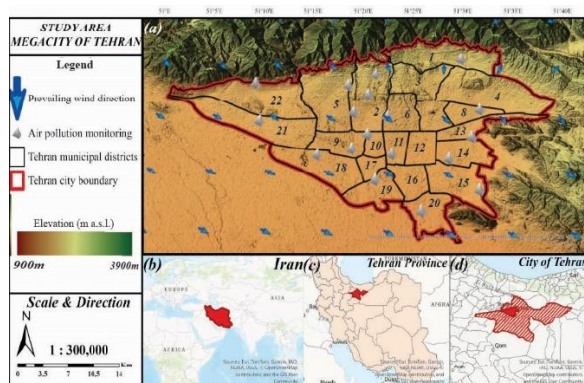


Figure 1. Geographic location of Iran within the Middle East (a), position of Tehran Province within the country (b), and administrative boundaries of the 22 municipal districts within the locations of ozone monitoring stations (c).

To construct a comprehensive set of predictors for the U-Net framework, multi-source atmospheric, biophysical, and geospatial datasets were integrated. Coarse-resolution tropospheric ozone concentrations (~1 km) were obtained from the Sentinel-5P/TROPOMI mission. Ground-based ozone measurements from Tehran’s Air Quality Monitoring Network were subsequently used to generate an interpolated reference surface for model calibration during spring 2020. Meteorological variables—including air temperature, wind components, relative humidity, and boundary-layer height—were derived from the ERA5 reanalysis, which provides physically consistent atmospheric fields suitable for data-driven modeling (Gauthier et al., 2022). Land-surface indicators such as NDVI, NDBI, and LST were extracted from Landsat-based products, while terrain-related datasets—including DEM, DSM, slope, and aspect—were derived from Copernicus elevation models. Additional chemical precursor information, most notably tropospheric NO₂ from Sentinel-5P, was incorporated to capture photochemical processes influencing ozone formation (He et al., 2023).

All datasets were uniformly reprojected to UTM Zone 39N and resampled to a 30-m spatial grid using cubic-spline interpolation to ensure consistent pixel alignment across data sources originally acquired at different spatial resolutions. Following reprojection and resampling, all predictor layers were clipped to Tehran’s municipal boundary. A SHAP-based feature-selection procedure was implemented to eliminate redundant or low-impact predictors, resulting in a final optimized multi-band stack consisting of 16 predictor variables. A detailed overview of the environmental, meteorological, topographic, and chemical datasets used in this study is presented in Table 1, which summarizes their respective sources, formats, and physical relevance to ozone dynamics.

Category	Dataset	Description	Source
Land Use and Urban Morphology	Land Cover	Land use classification of Tehran (urban, vegetation, bare, water)	ESA WorldCover
	CHM (Canopy Height Model)	Vegetation height structure derived from LiDAR	Copernicus DEM / GEDI
	ESA WorldCover	Global 10 m land cover product	ESA
	Road Density	Density derived from OSM road networks	OpenStreetMap
	Main Roads	Vector layer of primary and secondary roads	OpenStreetMap
Biophysical and Atmospheric Indicators	LST	Land Surface Temperature	MODIS
	NDVI	Normalized Difference Vegetation Index	MODIS
	NDWI	Normalized Difference Water Index	MODIS
	Air Temperature	Mean near-surface temperature	ERA5 Reanalysis (2023)
	Wind Speed & Direction Relative Humidity	Surface wind components Surface humidity (%)	ERA5 Reanalysis ERA5 Reanalysis
Topography and Terrain Morphology	DEM	Digital Elevation Model	Copernicus DEM
	DSM	Digital Surface Model	Copernicus
	Slope	Derived from DEM	GIS Analysis
	Aspect	Derived from DEM	GIS Analysis
Pollutant and Chemical Precursors	O ₃ (Interpolated Layer)	Spatially interpolated ozone concentration	Tehran Air Quality Monitoring Network
	NO ₂ (Tropospheric Column)	Tropospheric NO ₂ concentration	Sentinel-5P TROPOMI

Table 1. Description and sources of the spatial datasets used in the SUHI analysis

3. Methodology

The methodological workflow integrates deep-learning-based spatial downscaling with an interpretable feature-selection strategy to generate 30-m ozone concentration maps for the Tehran metropolitan region. The framework consists of three major components: (1) preprocessing and harmonization of multi-source spatial predictors, (2) SHAP-driven feature optimization, and (3) U-Net-based high-resolution ozone prediction.

3.1 Preprocessing and Harmonization of Predictors

All multi-source environmental, atmospheric, and topographic datasets—including land-surface indices, ERA5 meteorological parameters, Sentinel-5P chemical precursors, and Copernicus elevation derivatives—were standardized to a unified 30-m grid. Resampling through cubic-spline interpolation ensured spatial consistency among data layers originally acquired at different native resolutions (e.g., 10 m, 30 m, 1 km). All datasets were

reprojected to UTM Zone 39N and clipped to Tehran’s municipal boundary to prepare a geographically consistent predictor domain (Gauthier et al., 2022).

3.2 SHAP-Based Feature Optimization

Before model training, SHapley Additive exPlanations (SHAP) analysis was applied to quantify the marginal contribution of each predictor to ozone variability. This procedure enabled the systematic removal of low-impact variables—such as broad categorical land-cover layers and slope—while retaining high-influence predictors including DSM, DEM, LST, NDVI, wind vectors, and NO₂ concentrations (He et al., 2023). This feature-optimization step enhanced model stability, reduced noise propagation, and decreased computational cost.

Figure 2 presents the SHAP summary plot, highlighting the dominant role of topographic and thermal variables in shaping spatial ozone patterns in Tehran.

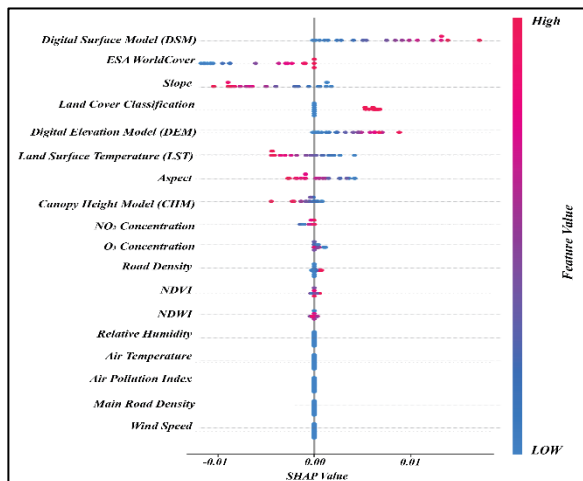


Figure 2. SHAP summary plot showing the relative importance of predictor variables in the optimized U-Net model.

3.3 U-Net Architecture for Atmospheric Downscaling

After feature optimization, the refined multi-band predictor stack was used to train a U-Net architecture specifically adapted for atmospheric downscaling. U-Net was selected due to its encoder–decoder structure and skip connections, which facilitate extraction of multiscale contextual information while preserving fine-scale spatial details (Li et al., 2020).

- The encoder path progressively compresses spatial information through convolutional blocks.
- The decoder path reconstructs high-resolution outputs using transposed convolutions.
- Skip connections link symmetric encoder–decoder layers, improving gradient propagation and retaining localized features.

A schematic representation of the architecture—from multi-source input layers to the final 30-m ozone output—is shown in Figure 3.

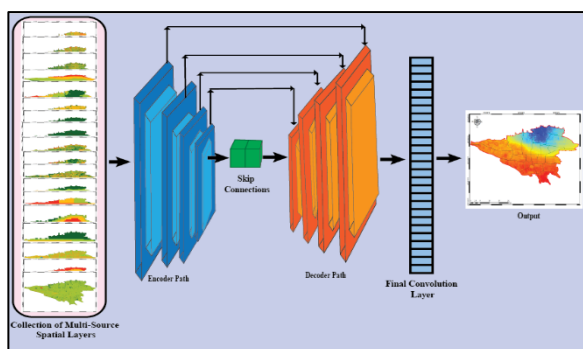


Figure 3. Structural overview of the U-Net architecture used for the 30-m ozone downscaling model, illustrating the encoder–decoder pathway and skip connections for multiscale spatial reconstruction.

3.4 Model Training and Evaluation

A supervised learning strategy was adopted, using the interpolated spring-2020 ozone surface as the reference layer. The dataset was split into training and validation subsets to ensure generalization. Model optimization employed the Adam optimizer with early stopping to prevent overfitting.

A post-training SHAP analysis was also conducted to interpret model behavior and identify the predictors exerting the strongest influence on spatial ozone variability. Results confirmed the significance of terrain morphology, land-surface temperature, vegetation indices, and NO₂ concentrations as key drivers of ozone formation in Tehran.

3.5 Integrated Workflow

Figure 4 provides a detailed illustration of the integrated end-to-end workflow used to generate 30-m ozone maps, highlighting the interaction between data preprocessing, feature optimization, U-Net training, and final output reconstruction. The process begins with data acquisition and preparation, where multi-source environmental, atmospheric, and chemical datasets from spring 2020 are collected and standardized. Gap-filled reference ozone surfaces derived from ground-based monitoring stations are then integrated to support supervised learning.

In the next stage, all predictor variables undergo normalization, removal of null and invalid values, and patch generation. The study area is divided into overlapping spatial patches (64×64 pixels) to improve training efficiency and ensure that local spatial variability is preserved during the convolutional learning process.

Following preprocessing, the SHAP module is applied to the initial multi-band predictor stack. SHAP value analysis identifies the predictors contributing most strongly to ozone variability, while low-impact or redundant variables are removed. This step produces an optimized feature set that enhances the stability and interpretability of the subsequent U-Net modeling process.

The refined predictor stack is then fed into the U-Net model. The network is trained using supervised learning, where the interpolated ozone surface acts as the ground-truth reference. The encoder–decoder structure allows the model to capture multiscale spatial features, while skip connections preserve fine-scale gradients essential for accurate ozone reconstruction.

Once the model is trained, pixel-level predictions are generated across the full Tehran metropolitan region. The reconstructed output is then reassembled into a continuous, spatially coherent map, combining all predicted patches into a final 30-m downscaled ozone product.

Overall, this workflow demonstrates a modular yet tightly interconnected system in which deep-learning modeling and SHAP-based feature interpretability reinforce each other. The integration of rigorous data preprocessing, optimized predictor selection, and a robust U-Net architecture results in physically meaningful, high-resolution ozone maps suitable for urban exposure modeling, atmospheric pollution analysis, and policy-oriented decision-making.

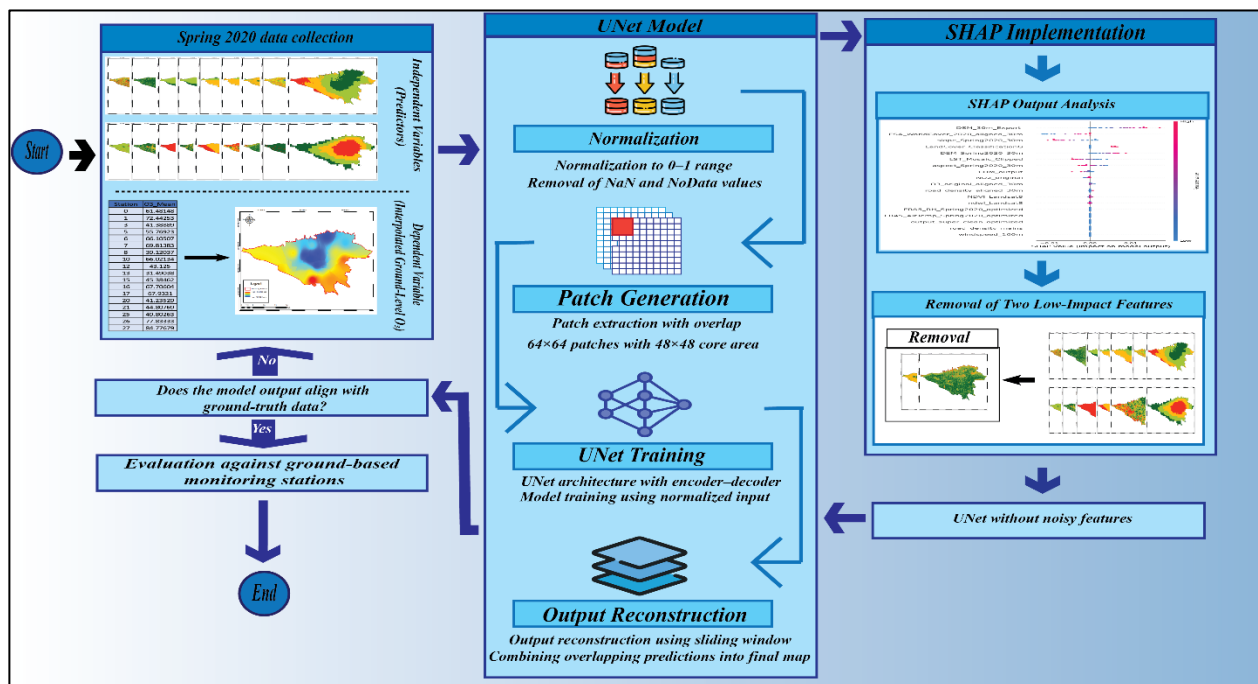


Figure 4. Overview of the complete methodological workflow, including data preprocessing, patch generation, SHAP-based feature optimization, U-Net training, and reconstruction of final high-resolution ozone maps.

4. Results and Evaluation

The optimized U-Net model demonstrated strong capability in reconstructing neighborhood-scale ozone patterns across the Tehran metropolitan region using the harmonized 30-m predictor dataset. Incorporating SHAP-driven feature selection substantially improved spatial consistency by removing redundant or weakly relevant predictors, thereby reducing edge artifacts and enhancing gradient continuity—particularly in areas with steep terrain variation (He et al., 2023). The optimized model produced smoother spatial transitions, sharper delineation of ozone hotspots, and stronger contrast relative to both the resampled Sentinel-5P product and the initial U-Net output.

During calibration, the model successfully reproduced Tehran’s characteristic north–south ozone gradient, with lower concentrations in the ventilated northern districts and higher values toward the central and southern low-lying basins. This spatial structure aligns with well-documented relationships between topography, atmospheric circulation, and emission density in Tehran (Ezimand & Kakroodi, 2019). Compared with the preliminary (non-optimized) U-Net configuration, the refined model preserved textural detail more effectively and achieved a more realistic representation of intra-urban gradients.

To quantitatively assess model performance, several statistical metrics—including R^2 , RMSE, MAE, correlation coefficients (R and ρ), and bias statistics—were computed by comparing the downscaled 30-m ozone outputs against

observations from Tehran’s ground-based monitoring stations. The results are summarized in Table 3, which also includes equivalent metrics for the original satellite dataset for comparison.

Dataset	R ²	RMSE (ppb)	MSE (ppb ²)	MAE (ppb)	R	ρ	Mean Bias (ppb)	Bias Range (ppb)
Downscaling model output	0.224	0.288	0.083	0.22	0.449	0.463	0.012	−0.15 to +0.18
Original satellite image	−1.614	0.421	0.177	0.354	−0.344	−0.327	0.123	−0.42 to +0.46

Table 3. Statistical evaluation of the downscaling model and the original satellite ozone product against ground-based ozone measurements in Tehran.

The downscaling model outperformed the raw Sentinel-5P observations across all statistical indicators. Notably, the U-Net output achieved lower RMSE, lower MAE, higher linear correlation, and substantially reduced bias. In contrast, the original satellite ozone product exhibited negative R² and moderate-to-high bias, indicating poor agreement with in situ measurements. These findings confirm that the optimized U-Net not only enhances the spatial resolution of ozone fields but also improves their quantitative consistency with ground-based observations.

Overall, the evaluation demonstrates that combining SHAP-based predictor refinement with U-Net downscaling yields a robust, interpretable, and physically consistent framework for enhancing coarse-resolution satellite-derived ozone products. The resulting 30-m maps provide substantially richer spatial detail and more reliable concentration estimates, making them suitable for neighborhood-scale exposure assessment, urban air-quality monitoring, and environmental planning applications.

5. Discussion and Conclusion

The findings of this study demonstrate that integrating SHAP-based feature optimization with a U-Net downscaling architecture provides a robust and interpretable framework for enhancing the spatial resolution of satellite-derived ozone products in complex urban environments. A key outcome is that systematically removing redundant or weakly informative predictors substantially improves model stability and reduces spurious spatial noise, as evidenced by the transition from preliminary to optimized outputs in the comparative spatial maps. This behavior aligns with previous research emphasizing the sensitivity of deep-learning ozone models to variable selection and predictor redundancy (He et al., 2023). By retaining only high-impact predictors—such as DSM, DEM, LST, NDVI, and NO₂—the optimized model concentrates its capacity on physically meaningful signals, thereby resolving coherent ozone gradients rather than fitting localized artifacts.

The model’s ability to reconstruct Tehran’s characteristic north–south ozone gradient further confirms that the proposed framework preserves the underlying physical processes governing ozone formation in topographically constrained megacities. Elevated northern districts experience stronger ventilation and lower precursor

accumulation, whereas central and southern basins tend to trap emissions and favor photochemical ozone production.

This pattern, previously documented in studies of Tehran’s air quality (Ezimeh & Kakroodi, 2019), is clearly reproduced in the optimized 30-m outputs, demonstrating that the deep-learning architecture is not simply interpolating the satellite signal but is effectively learning the interactions between terrain, land-surface properties, and atmospheric conditions.

The validation results reinforce this interpretation. The model performs well at both the point scale—through agreement with individual monitoring stations—and at the aggregated neighborhood scale across Tehran’s 22 municipal districts. This dual consistency is essential for operational applications, where both localized hotspots and broader intra-urban gradients must be captured reliably. The ability of the U-Net architecture to preserve fine-scale detail while maintaining large-scale structure represents a clear advantage over traditional statistical and simpler machine-learning approaches, which often struggle to balance local texture with regional atmospheric trends (Gauthier et al., 2022). These findings suggest that spatial–context-aware neural architectures, which explicitly incorporate neighborhood information through convolutional filters and skip connections, are particularly well suited for downscaling atmospheric pollutants in heterogeneous urban settings.

Another important contribution of this work lies in its strong emphasis on interpretability. Deep-learning models are frequently criticized for functioning as “black boxes,” making their internal decision processes opaque. By embedding SHAP analysis directly into the modeling workflow, this study provides explicit quantification of each predictor’s influence on the final ozone estimates. This transparency verifies that physically plausible drivers—such as elevation, surface temperature, vegetation, and NO₂—are indeed governing the model outputs rather than spurious correlations. Such interpretability enhances scientific credibility and increases the practical value of the results for environmental practitioners and policy-makers who require physically interpretable evidence to guide mitigation strategies. The joint emphasis on predictive accuracy and interpretability therefore distinguishes the proposed framework from many conventional deep-learning downscaling schemes.

Finally, the modular structure of the framework ensures its adaptability beyond the specific case examined here. Although the evaluation focused on spring 2020, the methodology is inherently transferable to other seasons and

years, provided comparable predictor datasets are available. Moreover, the same U-Net–SHAP design can be applied to other pollutants such as NO₂ or PM_{2.5}, as well as to multi-pollutant modeling where interactions among atmospheric species are important. Because the approach operates directly on satellite imagery and ancillary geospatial datasets, it is well suited for application in other megacities with complex terrain and limited monitoring infrastructure, offering a scalable tool for urban air-quality assessment.

In summary, this study demonstrates that SHAP-optimized U-Net downscaling can substantially enhance the spatial resolution and physical consistency of satellite-derived ozone fields, producing 30-m maps suitable for neighborhood-scale exposure assessment and urban environmental planning. The combination of high downscaling accuracy, cross-scale coherence, and model interpretability positions the proposed framework as a strong candidate for integration into operational urban air-quality monitoring systems and for supporting evidence-based policy interventions.

References

- Afarideh, F., Ramasht, M. H., & Mortyn, G. (2023). Air pollution and topography in Tehran. *Geografic*, 128(2), 157–170.
- An, T., Li, J., Lin, Q., & Li, G. (2024). Ozone formation potential related to the release of volatile organic compounds (VOCs). *Environmental Science: Atmospheres*, 4, 1229. <https://doi.org/10.1039/D4EA00091A>
- Chen, C.-C., Wang, Y.-R., Wang, F.-C., Shiu, Y.-S., Wu, C.-F., & Lin, T.-H. (2024). Estimating monthly NO₂, O₃, and SO₂ concentrations via an ensemble three-stage procedure with downscaled satellite remote sensing data and ground measurements. *Journal of Hazardous Materials*, 480, 136392. <https://doi.org/10.1016/j.jhazmat.2024.136392>
- Chen, J., Dong, H., Zhang, Z., & He, S. (2025). Ultra-high-resolution modeling of ground-level ozone for long-term exposure risk assessment driven by GTR-transformer. *Environment International*, 202, 109705. <https://doi.org/10.1016/j.envint.2025.109705>
- Cheng, S., Zhang, G., Yang, X., & Lei, B. (2024). A multiscale geographically weighted regression kriging method for spatial downscaling of satellite-based ozone datasets. *Frontiers in Environmental Science*, 11, 1267752. <https://doi.org/10.3389/fenvs.2023.1267752>
- de Foy, B., et al. (2022). Topography-driven air pollution dispersion in mountain megacities. *Atmospheric Environment*, 278, 119137. <https://doi.org/10.1016/j.atmosenv.2022.119137>
- Donzelli, G., & Suárez-Varela, M. M. (2024). Tropospheric ozone: A critical review of the literature on emissions, exposure, and health effects. *Atmosphere*, 15(7), 779. <https://doi.org/10.3390/atmos15070779>
- Ezimand, K., & Kakroodi, A. A. (2019). Prediction and spatio-temporal analysis of ozone concentration in a metropolitan area. *Ecological Indicators*, 103, 589598. <https://doi.org/10.1016/j.ecolind.2019.04.059>
- Gauthier Manuel, H., Mauny, F., Boilleaut, M., Ristori, M., Pujol, S., Vasbien, F., Parmentier, A.-L., & Bernard, N. (2022). Improvement of downscaled ozone concentrations from the transnational scale to the kilometric scale: Need, interest and new insights. *Environmental Research*, 210, 112947. <https://doi.org/10.1016/j.envres.2022.112947>
- Geddes, L. A., Eskes, H. M., Veefkind, J. P., Curier, L., Segers, A. J., & Boersma, K. F. (2022). Importance of satellite observations for high-resolution mapping of surface NO₂ and O₃: A case study in the Netherlands. *Remote Sensing of Environment*, 276, 113075. <https://doi.org/10.1016/j.rse.2022.113075>
- He, Z., et al. (2023). Integration of Shapley additive explanations with random forest: Application in environmental modeling. *Frontiers in Environmental Science*.
- Hu, W., et al. (2024). Urban heat island intensification and ozone formation in Asian megacities. *Science of the Total Environment*, 919, 170243. <https://doi.org/10.1016/j.scitotenv.2024.170243>
- Li, Z., He, Y., Zhang, S., & Li, M. (2020). Attention UNet++: A nested attention-aware U-Net for semantic segmentation. *IEEE Access*, 8, 142781–142790. <https://doi.org/10.1109/ACCESS.2020.3013142>
- Lu, C., Zhou, Z., Liu, H., Chen, X., Tan, Q., Wang, N., Yang, X., Huang, L., & Yang, F. (2024). An iteratively optimized downscaling method for city-scale air quality forecast emission inventory establishment. *Science of the Total Environment*, 954, 176824. <https://doi.org/10.1016/j.scitotenv.2024.176824>
- Mamić, L., & Pirotti, F. (2025). Harnessing open remote sensing data and machine learning for daily ground-level ozone prediction models: Spatio-temporal insights in the continental biogeographical region. *Atmospheric Pollution Research*, 16, 102514. <https://doi.org/10.1016/j.apr.2025.102514>
- Ponce-Bobadilla, A. V., et al. (2024). Practical guide to SHAP analysis: Explaining supervised machine learning models. *PLOS ONE*.
- Roldán, A., et al. (2021). Mountain–valley circulation impacts on ozone in Santiago. *Atmospheric Chemistry and Physics*, 21, 1158711603. <https://doi.org/10.5194/acp-21-11587-2021>
- Seguel, R. J., Mancilla, C. A., Rondanelli, R., Leiva, M. A., & Morales, R. G. E. (2013). Ozone distribution in the lower troposphere over complex terrain in Central Chile. *Journal of Geophysical Research: Atmospheres*, 118(5), 2309–2320. <https://doi.org/10.1002/jgrd.50293>
- Sherafati, L., Aghamohammadi Zanjirabad, H., & Behzadi, S. (2022). Spatio-temporal modeling of ozone distribution in Tehran, Iran, based on neural network and GIS. *Environmental Monitoring and Assessment*, 194(3), 205. <https://doi.org/10.1007/s10661-022-09840-x>
- Shetty, S., Hamer, P. D., Stebel, K., Kylling, A., Hassani, A., Berntsen, T. K., & Schneider, P. (2025). Daily high-resolution surface PM_{2.5} estimation over Europe by ML-based downscaling of the CAMS regional forecast. *Environmental Research*, 264, 120363. <https://doi.org/10.1016/j.envres.2024.120363>